

AN ANALYTICAL MODEL OF COMBUSTION OF SPENT OIL SHALE BLOCKS:
THE MODEL AND EXPERIMENTS

By

M-D. Ho, E. M. Suuberg^a and H. L. Toor
Department of Chemical Engineering, Carnegie-Mellon University, Pittsburgh, Pennsylvania 15213

INTRODUCTION

Oil shale, a potential source of liquid fuel, is a fine-grained, sedimentary rock composed of both organic and inorganic solid compounds. The production of liquid fuel from oil shale requires the retorting of the shale, in which oil and gas are destructively distilled from the shale rock, leaving behind a highly carbonaceous char within the spent shale matrix. The amount of char left depends on the richness of the raw shale. Typically, 23% by weight of the organic material originally present in the shale is left as char (1).

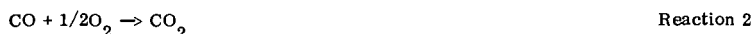
Combustion of this char could potentially provide all or part of the heat requirement for retorting of the shale (2). There have recently been several studies dealing with the combustion behavior of spent shale (2-8). Although char in shale is not pure carbon, most studies have treated it as carbon with reasonable success.

In the combustion of spent oil shale in an environment of air with other inert gases, there are three active components to be considered, O₂, CO₂ and CO and four major chemical reactions (9, 10), namely:

• Direct oxidation of the residual char, a process which is limited by the diffusion of oxygen and which creates an "unburned core".



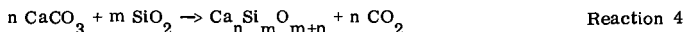
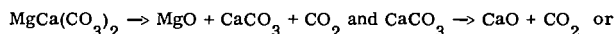
• Oxidation of CO



• CO₂-C gasification reaction



• Carbonate decomposition reactions^b



Therefore, the combustion of spent shale consists of two competing schemes: one is the direct oxidation of char; the other is the gasification of the char by CO₂ released from the carbonate decomposition reactions.

There have been several modeling studies of the combustion of spent shale in the presence of oxygen and nitrogen (2-7) which used the classical shrinking core model. This model assumes that the reaction rate is limited only by the internal diffusion of oxygen; hence, it neglects the other reactions (2, 3 and 4) which may play a major role at elevated temperature (above 875°K).

Mallon and Braun (7, 11) have included the decomposition and gasification reactions (3 and 4) in their model, but they treated the gasification reaction and the direct oxidation reaction independently and then superposed the two results. This approximation was inaccurate. Braun et al.

a. Present address: Division of Engineering, Brown University, Providence, Rhode Island 02912.
b. For the detail and kinetics of this reaction, see Manor et al (8).

(2) modeled gasification of spent oil shale blocks by steam and CO₂ but did not consider oxidation reactions. Their solution scheme involved solving differential equations numerically.

Our previous publication (Manor et al. (8)) offered a model which successfully predicted the combustion behavior of shale in nitrogen diluted air, but that model also required the numerical solution of differential equations.

The model that we present here is an improvement over the model of Manor et al. The major advantage of the new model lies in the simplicity of the closed form result which eliminates the necessity of cumbersome numerical solution of the differential equations. Our new model thus allows more convenient use of the single particle (or block) combustion model in the modeling of packed bed retorts. Experiments similar to those carried out earlier were used to extend the data.

DEVELOPMENT OF THE MODEL

Consider the burning sample shown schematically in Figure 1. We will use the assumptions that were employed by Manor et al. (8).

1. Mass transfer processes may be treated as pseudo-steady.
2. Only radial transport in a cylinder is considered.
3. Temperature is spatially uniform.
4. No significant pressure gradient exists within the shale.
5. The reaction of char with oxygen is fast enough to be lumped at the surface of the unburned core.
6. The gasification Reaction 3 occurs uniformly within the unburned core.
7. Carbonates decompose uniformly throughout the shale.
8. The bulk flow of all species out of the shale is dominated by the release of carbon dioxide from the decomposition of carbonates.
9. Fick's law holds for each component and all effective diffusivities are equal.

An additional assumption that allows the model to be treated analytically is that the oxidation reaction of carbon monoxide is instantaneous^a.

Transport Model

The formal statement of assumption 8 is:

$$N_t = R_4 (7r^2/2\pi r) = R_4 r/2 = G L y \quad 1)$$

where

$$L = C D_e / r_s$$

$$G = R_4 r_s^2 / (2 D_e C)$$

$$y = r/r_s$$

and where r_s is the radius of the cylinder. Other symbols are defined in the table of nomenclature.

The formal statement of assumption 9 is:

$$N_i = -C D_e dX_i/dr + X_i N_t \text{ or } N_i = -L dX_i/dy + X_i G L y, \quad i = \text{CO}, \text{CO}_2, \text{O}_2 \quad 2)$$

The species conservation equation for each component can be written as:

$$1/r d/dr (r N_i) = \sum_j \nu_{ij} R_j \quad 3)$$

where ν_{ij} is the stoichiometric coefficient of component i with respect to R_j . At the surface of the cylindrical sample ($r=r_s$ or $y=1$), external mass transfer resistance is taken into account by specifying:

$$N_{i,s} = (K_x + N_t) [2 Q / (K_x + 2Q)] X_{i,s} - K_x [2 Q / (K_x + 2Q)] S_{i,f} \quad 4)$$

- a. The measured CO/CO₂ ratio at the surface of the shale never exceeded 20% in the ignition stage and then declined very rapidly to a negligible value, therefore, we assume all CO is burned to CO₂ very quickly in the presence of oxygen. See also Manor et al. (8) for more detail.

where Q is the molar flow rate of sweeping gas per unit surface area of the sample. The new correction term, $[2Q/(K_x + 2Q)]$, is used to take into account the change in sweeping gas compositions due to the mass transfer to and from the sample. When the gas flow rate is very large, the correction term reduces to unity and is not required.

Define a pseudo-component concentration:

$$X_1 \equiv 1/2X_{CO} + X_{CO_2} + X_{O_2}, \quad N_{x_1} \equiv 1/2N_{CO} + N_{CO_2} + N_{O_2}$$

It follows from Equation 3 and the stoichiometry of the reactions that

$$1/r \, d/dr (r N_{x_1}) = R_4 \quad 5)$$

The substitution of Equation 2 into Equation 5 yields:

$$1/y \, d/dy (-y (dX_1/dy) + X_1 G y^2) = G \quad 6)$$

subject to the boundary conditions that, at the center of the sample, the flux is zero and at the surface of the sample, Equation 4 holds for pseudo-component 1.

Thus, Equation 6 can be solved to give:

$$X_1 = 1 + Kx/(Kx + G L) (X_{1,f} - 1) \exp((y^2 - 1) G/2) \quad 7)$$

which eliminates one unknown.

For the sake of convenience, we shall first consider the two regions of shale separately: the unburned core region and the product of shell layer.

Core Reaction Model

The core reaction model is similar to the one in Manor et al. (8), it is rederived here for the convenience of the reader. Within the unburned core section, the conservation equation for CO can be written as:

$$1/r \, d/dr (r N_{CO}) = 2 R_3 \quad 8)$$

with boundary conditions:

$$r = 0, \quad dX_{CO}/dr = 0; \quad r = r_c, \quad X_{CO} = X_{CO,c}$$

where r_c is the radius of the edge of the unburned core. Assumption 6 allows R_3 to be treated as position independent. Its value is evaluated at the average concentrations of reactants within the core. Therefore, Equation 8 can be integrated to give:

$$X_{CO} = (X_{CO,c} - B) \exp[(y^2 - y_c^2) G/2] + B$$

where

$$B = 2 R_3 / R_4 = R_3 (4GL/r_s)$$

Note that $X_{CO_2} = X_1 - 1/2X_{CO}$ in the core region, since $X_{O_2} = 0$ and the average mole fractions are:

$$\langle X_{CO} \rangle = (X_{CO,c} - B) \left[\frac{1 - \exp(-G y_c^2/2)}{G y_c^2/2} \right] + B \quad 9)$$

$$\langle X_{CO_2} \rangle = (X_{CO_2,c} - 1 + B/2) \left[\frac{1 - \exp(-G y_c^2/2)}{G y_c^2/2} \right] + 1 - B/2 \quad 10)$$

where

$$X_{CO_2,c} = X_{1,c} - 1/2 X_{CO,c}$$

It is assumed that C₂O-C gasification proceeds at a rate given by the equation suggested by Ergun (13)

$$R_3 = \frac{K_a G_c}{1 + \langle X_{CO} \rangle / K_{ex} \langle X_{CO_2} \rangle} \quad (\text{gmole/cm}^3 \text{sec}) \quad 11)$$

where $K_a = 4.5 \times 10^7 \exp(-24,500/T) + 3.75 \times 10^2 \exp(-16,000/T) \text{ sec}^{-1}$ (as suggested by Campbell and Burnham (9)). C_c is the molar concentration of char (gmole/cm³) and $K_{ex} = 138 \exp(-7,500/T)$ (from Ergun and Menster (14)).

Shell Transport and Reaction Model

In order to eliminate reaction terms in the conservation equation, let us again create a pseudo-component X₂, where

$$X_2 \equiv X_{O_2} - 1/2 X_{CO}, \quad N_{x_2} \equiv N_{O_2} - 1/2 N_{CO}$$

It follows that in the shell region,

$$1/r \, d/dr (r N_{x_2}) = 0 \quad 12)$$

and with Equation 2 and dimensionless variables,

$$1/y \, d/dy [-y (dX_2/dy) + X_2 G y^2] = 0 \quad 13)$$

Equations 12 and 13 can be integrated to give

$$y N_{x_2} = M \quad 14)$$

and

$$X_2 = M/L F(y, y_c) \exp(G y^2/2) + X_{2,c} \exp[G/2(y_c^2 - y^2)] \quad 15)$$

where:

$$X_{2,c} = X_{O_2,c} - 1/2 X_{CO,c}, \quad F(y, y_c) = \int_{y_c}^y \frac{\exp(-G\tau^2/2)}{\tau} \, d\tau$$

and M is an integration constant. At y=1, Equation 4 is used as the other boundary condition.

Since we have assumed that the oxidation reaction of carbon monoxide is instantaneous, it follows that the coexistence of carbon monoxide and oxygen is not allowed and the flame front at which all the oxidation reactions occur is assumed to be infinitely thin.

The flame front occurs either at the core surface, case 1, or out of the core surface (i.e., at r>r_c), i.e., case 2.

Case 1: Flame Front at the Core Surface

In this case, oxygen flux to the core surface will be consumed both by the reaction with carbon monoxide produced in the core and by the direct oxidation of char, i.e.,

$$-N_{O_2,c} = (R_1 + R_3) r_c / 2$$

where

$$R_1 = K_1 C_c X_{O_2,c}$$

and the value of K_1 is provided by Sohn and Kim (10) as $1.503 \times 10^7 \exp(-11102/T) \text{ sec}^{-1}$. (In Manor et al. (8), K_1 was assumed to be infinitely large.)

Since oxygen is present at the core surface in this case, we can assume $X_{CO,c}$ and $N_{CO,c}$ to be zero, which requires

$$X_{2,c} = X_{O_2,c} \text{ and } M = y_c N_{O_2,c}.$$

Therefore, we can calculate the oxygen flux by solving Equation 15 to get:

$$N_{O_2,s} = N_{x_2,s} = \frac{K_x X_{O_2,f}^{-K_x + G L} X_{O_2,c} \exp((1-y_c^2)G/2)}{(K_x + 2Q)/2Q + (G + K_x/L) F(1, y_c) \exp(G/2)} \quad (16)$$

where

$$X_{O_2,c} = \frac{K_x X_{O_2,f} - R_3 r_s y_c^2 / 2 [(K_x + 2Q)/2Q + (G + K_x/L) F(1, y_c) \exp(G/2)]}{K_1 C_c r_s y_c^2 [(K_x + 2Q)/2Q + (G + K_x/L) F(1, y_c) \exp(G/2)] + (K_x + G L) \exp((1-y_c^2)G/2)}$$

Case 2: Flame Front Out of Core Surface

In case 2, the flame front is being pushed outward by carbon monoxide, so oxygen cannot reach the core surface and $X_{2,c}$ must be less than zero, since $X_{2,c} = 1/2 S_{CO,c}$

Note that since

$$N_{O_2,c} = 0, N_{x_2,c} = -1/2 N_{CO,c},$$

a mass balance around the core surface gives:

$$N_{CO,c} = R_3 r_c \quad (17)$$

Using Equations 14 and 17, we can get

$$M = -R_3 r_s y_c^2 / 2 \quad (18)$$

Equations 15 and 18 allow us to compute the value of $X_{2,c}$ as:

$$X_{CO,c} = -2X_{2,c} = \frac{-2K_x X_{O_2,f} + r_s y_c^2 R_3 ((K_x + 2Q)/2Q + (G + K_x/L) F(1, y_c) \exp(G/2))}{(G L + K_x) \exp(G/2 (1-y_c^2))} \quad (19)$$

Model Solution

Note that in the core region, if we substitute Equations 9 and 10 into Equation 11, R_3 can be solved as a function of $X_{CO,c}$, while in the reacted shell region $X_{CO,c}$ is either zero in case 1, or can be obtained from Equation 19 as a function of R_3 in case 2. Simultaneous solution of these two regions gives the following equation:

$$R_3 = \sqrt{\frac{(K_3 K_5 K_{ex}^2 - 2K_3 K_4 K_5 K_{ex}^2 + (K_4 K_{ex})^2 - 2K_2 K_{ex} (K_3 K_5 + K_4) + 4K_1 K_4 K_5 K_{ex} + K_2^2)}{+ K_2 - K_3 K_5 K_{ex} - K_4 K_{ex}} / (4K_1 - 4K_3 K_{ex})} \quad (20)$$

where

$$K_1 = C_4 - 2 C_4 C_5 + 2 C_1 C_5$$

$$K_2 = 2 C_2 C_5$$

$$K_3 = C_1 C_5 + 1/2 C_4 - C_4 C_5$$

$$K_4 = 1 + 2 C_3 C_5 - 2 C_5$$

$$K_5 = 2 K_{ab} \rho_c / MW_c$$

and

$$C_1 = 0 \quad (\text{Case 1})$$

or

$$r_s y_c^2 \exp(G y_c^2) [F(1, y_c) / L + \exp(-G/2)(kx + 2Q) / 2Q / (k_x + GL)] \quad (\text{Case 2})$$

$$C_2 = 0 \quad (\text{Case 1})$$

or

$$2X_{O_2, f} \exp(G/2(y_c^2 - 1)) [k_x / (GL + k_x)] \quad (\text{Case 2})$$

$$C_3 = 1 + \exp(G/2(y_c^2 - 1)) [k_x / (GL + k_x)] (X_{O_2, f} + X_{CO_2, f} - 1) \quad (\text{Case 1})$$

or

$$1 + \exp(G/2(y_c^2 - 1)) [k_x / (GL + k_x)] (2X_{O_2, f} + S_{CO_2, f} - 1) \quad (\text{Case 2})$$

$$C_4 = r_s / 2GL$$

$$C_5 = \left[\frac{1 - \exp(-G y_c^2 / 2)}{G y_c} \right]$$

Thus, R_3 can be obtained from Equation 20 and all the other quantities desired, such as

$$N_{O_2, s}$$

(the oxygen consumption rate) and dy/dt (the rate of shrinkage of the core) can be calculated in a straightforward fashion. A trial and error calculation procedure is used to determine whether case 1 or case 2 is true. This model is then integrated numerically only over time, with the reaction rates and temperature recalculated at each time step.

PHYSICAL PROPERTIES

In the model calculation, the temperature is calculated from

$$\sum_s C_p (dT_s/dt) = h S \Delta T + \sum R_i \Delta H_i$$

where the heat capacity is:

$$C_p = 0.72 + 7.7 \times 10^{-4} T_s^2 / (T_s + 300) \text{ J/gm-K}$$

and the heat transfer coefficient ^a is:

$$h = 9.76 \times 10^{-4} + 2.48 \times 10^{-6} (T_s - 755) \text{ W/cm}^2\text{K}$$

The temperature difference ΔT in the heat loss term is actually measured in our experiments, it usually maintains a constant value throughout an experiment due to the configuration of the reactor.

A general correlation based on a random pore model (15) allows us to estimate the effective diffusivity of spent oil shale as:

$$D_e = \epsilon^2 D_{O_2, \text{air}}$$

where ϵ is the porosity and

$$D_{O_2, \text{air}}$$

is the bulk binary diffusivity of oxygen in air. Note that there are no adjustable parameters in the above equation. This approach is a modification of that used by Manor et al.

For the purpose of prediction, porosity, char concentration and shale grade can be conveniently estimated from shale density using correlations in the literature (16, 17).

Smith provided a theoretical relationship between density and oil yield for oil shale (17) and he supported his prediction with experimental results. The correlation was found to be very good in our experiments.

The data on the carbonaceous char contents of spent shales was gathered by Stanfield et al. (1) and his result can be correlated as follows:

$$W_c = 1.903 \times 10^{-3} + 2.283 \times 10^{-4} A$$

where W_c is the char density as percentage of the raw shale density (not weight fraction of the spent shale, as Dockter and Turner stated) and A is the shale grade in liters of oil per ton. The initial porosity of the spent shale returned to 750°K can also be estimated with Tisot's data which is correlated by Dockter and Turner (5):

$$\epsilon = 0.111 + 1.55 \times 10^{-3} A + 1.23 \times 10^{-5} A^2$$

EXPERIMENTAL VERIFICATION

The analytical model gives results very close to the numerical model of Manor et al., which agreed reasonably well with the experimental data reported earlier. In addition, a number of new experiments were carried out to further test the validity and applicable range of the model. The experimental conditions used were similar to the earlier one (8). Colorado oil shales were machined into cylinders and retorted in a furnace in nitrogen to a maximum temperature of 750°K. The combustion was then initiated by switching the sweep gas from nitrogen to air or nitrogen diluted air. Heat transfer to and from the furnace wall was minimized by controlling the furnace wall to within two °K of the shale surface temperature.

The effects of shale grades (from 40 to 229 liter/ton), cylinder sizes (from 1 cm to 10 cm

a. The heat transfer coefficient sometimes has been adjusted to account for non-ideal temperature distribution in the furnace during rapid temperature rise.

in diameter) and feed gas oxygen concentration (from 5% to 21%) were examined. It was found that this model adequately accounts for these effects in the testing range. Shown in Figure 2 is the comparison of experimental and model prediction of average temperatures and dimensionless reaction rates of rich shale cylinders (208 liter/ton) of two different sizes (3.5 cm, and 9.3 cm in diameter) in 13.5% oxygen plotted against dimensionless time. A 5 cm sample from the same piece of rock was also tested against the model with similar success but the result was excluded from the figure to avoid crowding. It can be seen from Figure 2 that the two different size samples give very similar curves on a dimensionless time scale (the 5 cm sample gave similar curves), but other grades of shale do not scale this way.

Various sizes (1 cm, 3.4 cm, 5.1 cm and 9.7 cm diameters) of 104 liter/ton shale have also been used and the model also predicted the combustion behavior successfully. In Table I, we compare measured and predicted total burn out times for these samples.

TABLE I

BURN OUT TIME FOR MEDIUM GRADE SHALE^a (104 LITER/TON) OF FOUR DIFFERENT SIZES: EXPERIMENTS AND MODEL PREDICTION

| Expt. No. | Shale Diameter | O ₂ % | Burn Out Time | |
|-----------|----------------|------------------|---------------|----------|
| | | | Expt. | Model |
| 55 | 9.7 cm | 21% | 660 min. | 670 min. |
| 65 | 5.1 cm | 15% | 340 min. | 330 min. |
| 67 | 3.4 cm | 15% | 160 min. | 163 min. |
| 69 | 1.0 cm | 15% | 20 min. | 22 min. |

- a. Important parameters used are: Initial porosity = 30%, carbon density = 0.06 gm/cm³, spent shale density = 1.87 gm/cm³.

CONCLUSION

An analytical model satisfactorily predicts the combustion behavior of spent oil shale blocks. The only additional assumption besides those employed by Manor et al. (8) is that the oxidation reaction of carbon monoxide is instantaneous.

ACKNOWLEDGMENTS

We wish to thank Occidental Petroleum Corporation and Rio Blanco Oil Shale Company for supplying the oil shale used in this work.

NOMENCLATURE

| | |
|----------------|--|
| A | shale grade, liter/ton |
| B | constant defined as $2R_3/R_4$, dimensionless |
| C | molar concentration in gas phase, gmole/cm ³ |
| C _c | molar concentration of char in shale, gmole/cm ³ |
| C _i | constants, defined below Equation 20 |
| C _p | heat capacity of the shale, J/gm-K |
| D _e | effective diffusivity of gases in the shale, cm ² /sec |
| G | constant = $R_4 r_s^2 / 2CD_e$, dimensionless |
| h | heat transfer coefficient, W/cm ² K |
| K _i | constants, defined below Equation 20 |
| K _x | mass transfer coefficient, gmole/sec-cm ² |
| L | constant = CD_e / r_s , gmole/sec-cm ² |
| N _t | net molar flux anywhere within the sample, gmole/sec-cm ² |

| | |
|-----------------------|--|
| N_i | molar flux of any species i , gmole/sec-cm ² |
| Q | the molar feed rate of gas per unit surface area of the sample |
| R_1 | molar rate of the direct oxidation of char, gmole/sec-cm ³ |
| R_2 | molar rate of the oxidation reaction of CO, gmole/sec-cm ³ |
| R_3 | molar rate of CO ₂ -C gasification reaction, gmole/sec-cm ³ |
| R_4 | molar rate of release of CO ₂ from carbonate decomposition reactions, gmole/sec-cm ³ |
| r | radial position within shale sample, cm |
| r_s | the radius of the shale sample, cm |
| S | surface area of sample per unit volume, cm ⁻¹ |
| T_s | shale temperature, K |
| ΔT | temperature difference between the shale and the sweeping gas |
| ΔH_j | heat of reaction j , J/gm-K |
| W_c | weight fraction of carbonaceous char in raw shale, dimensionless |
| x_i | mole fraction of any species i , i =CO, O ₂ , CO ₂ , dimensionless |
| $\langle x_i \rangle$ | average mole fraction of species i in the core region, i =CO ₂ , CO, dimensionless |
| y | $=r/r_s$, normalized radial position within sample, dimensionless |
| ϵ | porosity, dimensionless |

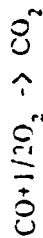
SUBSCRIPTS

| | |
|-----|---------------------------------------|
| c | value at the core edge |
| f | value in the feed stream |
| i | CO, O ₂ or CO ₂ |
| s | value at the shale surface |

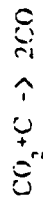
Figure 1: Reaction scheme. This diagram indicates the locations at which the four main reactions occur, and indicates the sources and sinks of the three key reactant species.



Reaction 1



Reaction 2



Reaction 3



Reaction 4

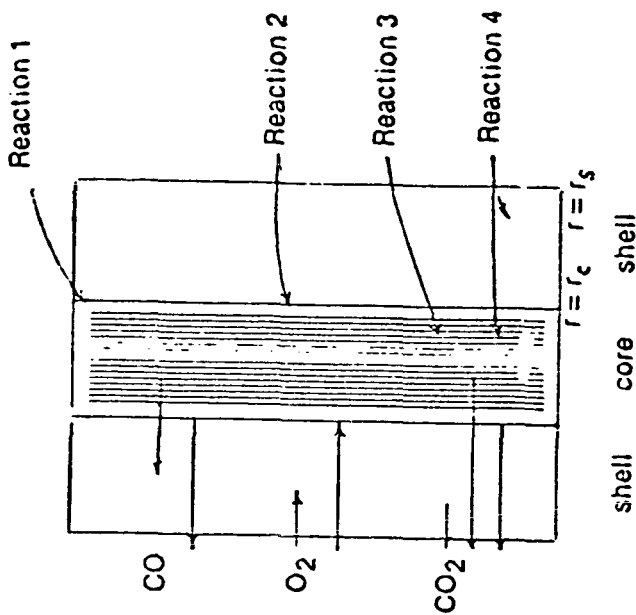
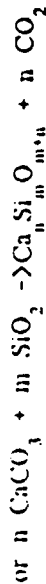
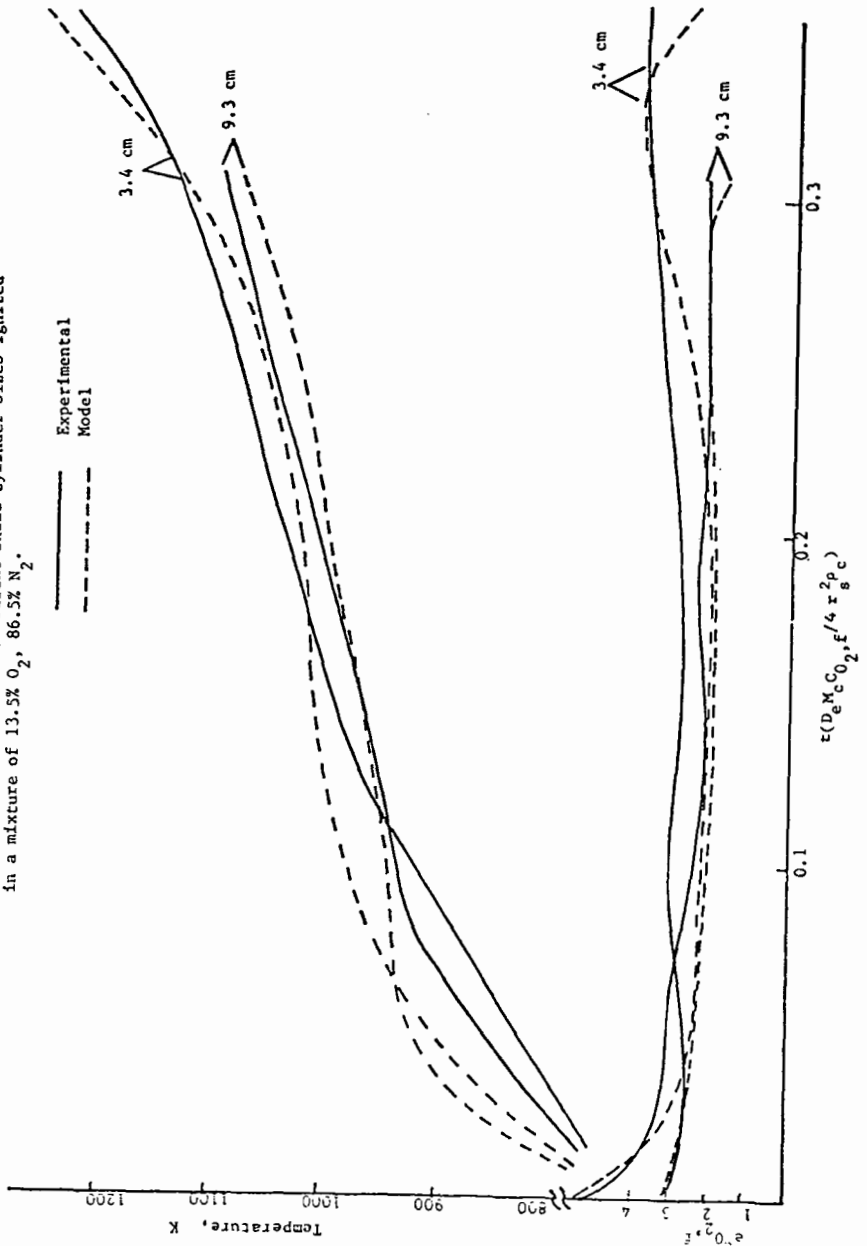


Figure 2: Comparisons of experimental results and model predictions. Average temperatures and dimensionless reaction rates vs. dimensionless time. Two different shale cylinder sizes ignited in a mixture of 13.5% O₂, 86.5% N₂.



LITERATURE CITED

- (1) Stanfield, K. E. , Frost, I. E. , Mcauley, W. S. and Smith, W. S. , "Properties of Colorado Oil Shale", U. S. Bureau of Mines, RI 4825 (1951).
- (2) Dockter, L. , "Combustion of Oil-Shale Carbon Residue", AICHE Symp. Series, Vol. 72, No. 155 , p. 24 (1975).
- (3) Huang, E. T. S. , "Retorting of Single Oil-Shale Blocks with Nitrogen and Air", SPE Journal, p. 331 (October 1977).
- (4) Thomson, W. J. and Soni, Y. , "Oxidation of Oil Shale Char", In Situ, Vol. 4, No. 1, p. 61 (1980).
- (5) Dockter, L. and Turner, T. F. , "Combustion Rates for Oil Shale Carbonaceous Residue", In Situ, Vol. 2, No. 3, p. 197 (1978).
- (6) Duvall, J. J. and Tyner, C. E. , "Laboratory and Modeling Studies of the Combustion Retorting of Large Clocks of Oil Shale", Tech. report, Sandia Laboratories (1979).
- (7) Mallon, R. and Braun, R. , "Reactivity of Oil Shale Carbonaceous Residue with Oxygen and Carbon Dioxide", Quarterly of the Colorado School of Mines, Vol. 71, No. 4, Proceedings of the 9th Oil Shale Symp. (1976).
- (8) Manor, Y. , Suuberg, E. M. , Ho, M. and Toor, H. L. , "The Ignition and Combustion Behavior of Spent Shale Particles", in 19th Interntl. Symp. on Combustion, The Combustion Institute, Pittsburgh, PA, p. 1093 (1982).
- (9) Campbell, J. H. and Brunham, A. K. , "Reaction Kinetics for Modeling Oil Shale Retorting", In Situ, Vol. 4, No. 1 (1980).
- (10) Sohn, H. Y. and Kim, S. K. , "Intrinsic Kinetics of the Reaction between Oxygen and Carbonaceous Residue in Retorted Oil Shale", Ind. Eng. Chem. , Process Design and Development, Vol. 19, No. 4, p. 550 (1980).
- (11) Braun, R. L. , "Mathematical Modeling of Modified In-Situ and Aboveground Oil Shale Retorting", Tech. report UCRL-53119, Lawrence Livermore Laboratory (1981).
- (12) Braun, R. L. , Mallon, R. G. and Sohn, H. Y. , "Analysis of Multiple Gas-Solid Reactions during the Gasification of Char in Oil Shale Blocks", Tech. report UCRL-85279, Lawrence Livermore Laboratory (April 1981).
- (13) Ergun, S. , "Kinetics of Reaction of Carbon Oxidide with Carbon", Journal of Physical Chem. , Vol. 60, p. 480 (1956).
- (14) Ergun, S. and Menster, M. , "Reaction of Carbon with CO₂ and Steam", in Chem. and Physics of Carbon, P. L. Walker, ed. , p. 203 (1965).
- (15) Smith, J. M. , Chem. Engineering Kinetics, McGraw-Hill Co. , p. 466 , 3rd ed. (1981).
- (16) Tisot, R. , "Alterations in Structure and Physical Properties of Green River Oil Shale by Thermal Treatment", J. Chem. Eng. Ref. Data, Vol. 12, p. 405 (1967).
- (17) Smith, J. W. , "Theoretical Relationship Between Density and Oil Yield for Oil Shales", Tech. report R17248, Bureau of Mines (April 1969).